ISSN: 2641-6336
Annals of
Biostatistics & Biometric Applications
DOI: 10.33552/ABBA.2025.06.000641
Iris Publishers

Research Article

The Kinetics of Reactions in the Mechanism of Ultraviolet Degradation of H_2S Combined with the Non-Appearance of O_2 Using the Homotopy Perturbation Method

Salahuddin[1]*, Sreelatha Devi V[2] and Saranya K[3]

[1]Department of Mathematics, College of Science, Jazan University, Kingdom of Saudi Arabia

[2]Department of Mathematics, Saveetha School of Engineering, India

***Corresponding author:** Salahuddin, Department of Mathematics, College of Science, Jazan University, Jazan-45142, P.O. Box 114, Kingdom of Saudi Arabia

Received Date: May 16, 2025
Published Date: June 09, 2025

Abstract

The presence of hydrogen sulphide has hampered the development of biogas energy. Traditional hydrogen sulphide photodegradation occurs in the presence of oxygen. However, this is inappropriate for biogas desulfurization and should be avoided. As a result, the current study is the first to investigate the theoretical UV degradation of H_2S in the absence of oxygen. First, a theoretical model of H_2S photodegradation was developed using the homotopy perturbation method, which included models of gas flow distribution and photoreactor radiation kinetics, mass balance, and degradation rate calculation. The impact of parameters such as H_2S mass and gas retention duration on the photodegradation rate was then investigated to validate the mathematical model. Furthermore, the rate of H_2S photodegradation increased as the retention time increased. The analytical results matched the experimental results extremely well, indicating that the mathematical model can be used to simulate H_2S photodegradation.

Keywords: Mathematical modelling; H_2S photodegradation; renewable energy techniques; nonlinear equations; and the homotopy perturbation method

Introduction

Anaerobic digestion, which is regarded as the most important strategy for producing renewable energy from biomass to recover clean biogas fuel, see [1], produces hydrogen sulphide [H_2S], which contains 0.3%–0.4% of the material CH_4 and CO_2, see [2]. H_2S is a foul acid gas with the potential to cause significant corrosion in equipment, instruments, and pipelines. Furthermore, H2S has a negative impact on people's health and the environment. When the biogas is used for energy (burning, generating power, etc.), the H_2S in it is converted to SO_2, which may significantly worsen air pollution (see [3]). Thus, the presence of H_2S impedes the promotion of biogas energy, and H2S must be extracted from biogas using efficient methods. H_2S techniques include biological, chemical, physical, and combinatorial technologies. The direct decomposition of H_2S to produce sulphur and hydrogen is a research topic for both domestic and international researchers because it allows for the recycling of hydrogen energy while also efficiently managing the H_2S pollution generated during the processing of coal, oil, gas, and minerals. Thermal [4,5], electrochemical [6], photocatalytic [7-9], and plasma degradation [10,11] are the primary H2S degradation processes that produce hydrogen and sulphur. Photocatalytic H_2S degradation is the most promising technique available today due to its high treatment efficacy and reaction movement [12] (Figure 1-3).

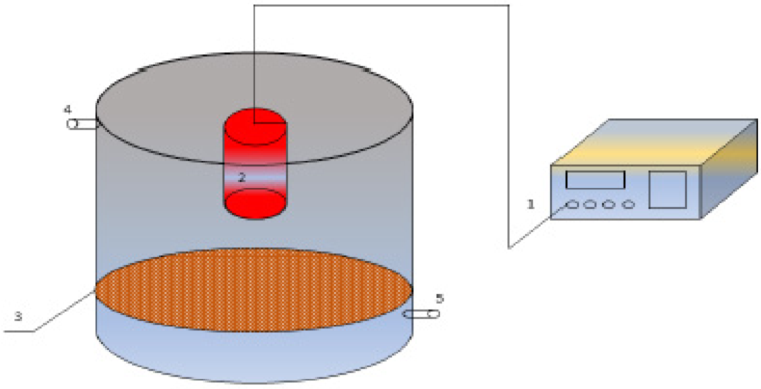

Figure 1: H2S photodegradation reactor: 1. Generator with High Frequency, 2. Distribution of Gas Equipment 3. Electrodeless VUV Lamp, 4. Gas Outlet, 5. Gas Inlet.

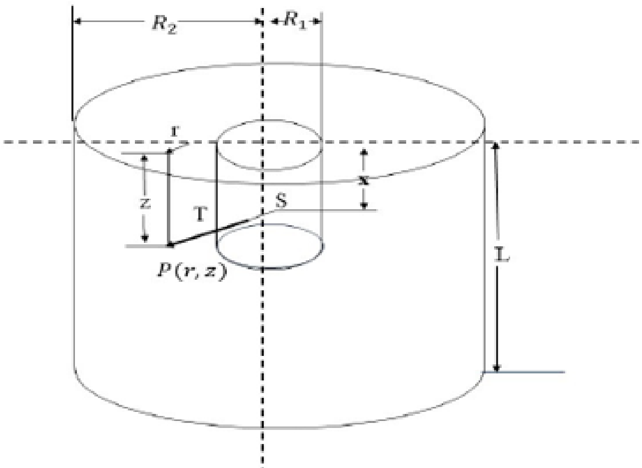

Figure 2: Cylindrical light source and Cylindrical photoreactor.

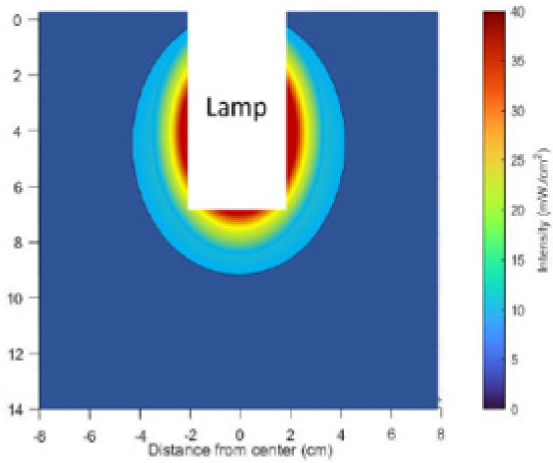

Figure 3: The distribution of light intensity within the photoreactor.

Mathematical Formulation of the Problem

Wilson et al. [13] investigated the direct photodegradation of hydrogen sulphide (H_2S) in the approaching Ultraviolet (UV) band. Photons with wavelengths below 270 nm can initiate degradation of H2S, resulting in the formation of hydroxyl radicals (H·) and sulfhydryl radicals (SH·). Moreover, further photon exposure, particularly with wavelengths less than 230 nm, facilitated the transformation of SH· into H· and sulphur radicals (S·), as confirmed by experimental evidence (1), and (2). These reactions demonstrate the complex interplay between H_2S and UV radiation, focusing on the formation of reactive intermediates such as radicals and their subsequent reactions with oxygen and other environmental species. Further research into these reaction pathways is critical for understanding the fate and impact of H_2S photodegradation in various environmental settings.

$$H_2S + h\nu(\lambda \le 270\,nm) \rightarrow H. + SH. \quad (1)$$

$$HS. + h\nu(\lambda \le 230\,nm) \rightarrow H. + S \quad (2)$$

$$H. + H_2S \rightarrow H_2 + HS. \quad (3)$$

$$H. + H. \rightarrow H_2 \quad (4)$$

$$H. + HS. \rightarrow H_2 + S \quad (5)$$

$$HS. + HS. \rightarrow S + H_2S \quad (6)$$

The degradation rate equation for each intermediate during the photodegradation of hydrogen sulphide in the absence of oxygen can be determined using the relevant literature, the Technology's chemical dynamics database, and the National Institute of Standards based on (1), (2), (3), (4), (5), and (6), respectively. As a photon is presented in (1) and (2), the rate constants are denoted by $kobs_1$, $kobs_2$, k_3, k_4, k_5, and k_6. The reaction rates of each component can be expressed using the equations below:

$$\frac{d[H_2S]}{dt} = -k_{obs1}[H_2S] - k_3[H_2S][H.] + k_6[SH.] \quad (7)$$

$$\frac{d[H.]}{dt} = k_{obs1}[H_2S] + k_{obs2}[SH.] - k_3[H_2S][H.] + k_4[H.]^2 - k_5[SH.][H.] \quad (8)$$

$$\frac{d[SH.]}{dt} = k_{obs1}[H_2S] + k_{obs2}[SH.] - k_5[SH.][H.] - k_6[SH.]^2 \quad (9)$$

$$\frac{d[H_2]}{dt} = k_3[H_2S][H.] + k_4[H.]^2 + k_5[H.][SH.] \quad (10)$$

$$\frac{d[S]}{dt} = k_{obs2}[SH.] - k_5[SH.][H.] - k_6[SH.]^2 \quad (11)$$

The initial conditions are given below:

$$\begin{aligned} &t = 0,\ H_2S = H_2S_{ini} \\ &t = 0,\ H. = H._{ini} \\ &t = 0,\ SH. = SH._{ini} \\ &t = 0,\ H_2 = H_{2ini} \\ &t = 0,\ S = S_{ini} \end{aligned} \quad (12)$$

and the boundary conditions are

$$\begin{aligned} &t = 0,\ H_2S = 0 \\ &t = 0,\ H. = 0 \\ &t = 0,\ SH. = 0 \\ &t = 0,\ H_2 = 0 \\ &t = 0,\ S = 0 \end{aligned} \quad (13)$$

Citation: Salahuddin*, Sreelatha Devi V and Saranya K. The Kinetics of Reactions in the Mechanism of Ultraviolet Degradation of H_2S Combined with the Non-Appearance of O_2 Using the Homotopy Perturbation Method. Annal Biostat & Biomed Appli. 6(4): 2025. ABBA.MS.ID.000641. **DOI:** 10.33552/ABBA.2025.06.000641.

Approximate Analytical Representation for the Concentration of H_2S Photodegradation and the Corresponding Reaction Rate Equations for H_2S, H, SH., H_2, And S Using HPM

Many researchers in engineering and physics have recently used the Homotopy perturbation method to solve a wide range of nonlinear problems [14-19]. This method combines a conventional perturbation scheme with topology. J. H. He, used the Homotopy perturbation method to solve the light hill equations [20], Duffing equations [21], and Blasius equations [22]. This method is notable for its efficiency, precision, and applicability. The Homotopy perturbation method uses the surrounding parameter p as a small parameter, and (Appendix A) it only takes a few duplications to find an asymptotic result. Using HPM (Appendix B), analytical expressions for the concentrations of H_2S, H., SH., H_2, and S are obtained using the homotopy perturbation method from these equations, giving the following results:

(Calculation was provided in the Supplementary Materials)

$$[\mathrm{H_2S}]t = c_1 e_1^{-at} + \frac{1}{c_4}\left[(\mathrm{L}_1 - \mathrm{L}_4 t)e_1^{-at} - \mathrm{L}_2\, e_1^{-at-bt} + \mathrm{L}_3\, e_1^{-2at} + c_{18} e_1^{-2bt}\right] \tag{14}$$

$$\begin{aligned}
[\mathrm{H.}]t = {} & \mathrm{c}_3\, e_1^{-at} + e_1^{-bt} - \mathrm{c}_2 + \frac{a}{\mathrm{c}_4}\left[\begin{array}{l} \mathrm{L}_1 \dfrac{e_1^{-at}}{-a} - \mathrm{L}_4\left(\mathrm{t}\dfrac{e_1^{-at}}{-a} - \dfrac{e_1^{-at}}{a^2}\right) - \mathrm{L}_2 \dfrac{e_1^{-(a+b)t}}{-(a+b)} \\ + \mathrm{L}_3 \dfrac{e_1^{-2at}}{-2a} + c_{18} \dfrac{e_1^{-2bt}}{-2b} \end{array}\right] + \\
& \frac{b}{\mathrm{p}_{98}}\left[\begin{array}{l} \mathrm{A}_1 \dfrac{e_1^{-2bt}}{-2b} - \mathrm{A}_2 \dfrac{e_1^{-bt}}{b} + \left(\mathrm{p}_{43} - \mathrm{p}_{71} + \mathrm{p}_{91}\right)\left(\mathrm{t}\dfrac{e_1^{-bt}}{-b} - \dfrac{e_1^{-bt}}{b^2}\right) \\ + \left(\mathrm{A}_3 + \mathrm{A}_6\right)\dfrac{e_1^{-(a+b)t}}{-(a+b)} - \mathrm{A}_4 \dfrac{e_1^{-at}}{-a} + \left(\mathrm{p}_{16} - \mathrm{p}_{44} + \mathrm{p}_{72}\right)\left(\mathrm{t}\dfrac{e_1^{-at}}{-a} - \dfrac{e_1^{-at}}{a^2}\right) \end{array}\right] \\
& - k_3\, \mathrm{c}_1\mathrm{c}_3 \frac{e_1^{-2at}}{-2a} + \mathrm{c}_1\, k_3 \frac{e_1^{-(a+b)t}}{-(a+b)} - \mathrm{c}_1\mathrm{c}_2\, k_3 \frac{e_1^{-at}}{-a} \\
& + k_4\left[\mathrm{c}_3^{\,2} \frac{e_1^{-2at}}{-2a} - 2\,\mathrm{c}_3 \frac{e_1^{-(a+b)t}}{-(a+b)} + 2\,\mathrm{c}_2\mathrm{c}_3 \frac{e_1^{-at}}{-a} + 2\,\mathrm{c}_2 \frac{e_1^{-bt}}{b} - \frac{e_1^{-2bt}}{2b} + \mathrm{c}_2^{\,2}\mathrm{t}\right] \\
& + k_5\left[\mathrm{A}\frac{e_1^{-(a+b)t}}{(a+b)} + \mathrm{Ac}_3 \frac{e_1^{-2at}}{2a} - \mathrm{Ac}_2 \frac{e_1^{-at}}{-a} + \mathrm{Bc}_3 \frac{e_1^{-(a+b)t}}{(a+b)} - \mathrm{Bc}_2 \frac{e_1^{-bt}}{b} + \mathrm{B}\frac{e_1^{-2bt}}{2b}\right]
\end{aligned} \tag{15}$$

$$[\mathrm{SH.}]t = \mathrm{A}\, e_1^{-at} + \mathrm{B}\, e_1^{-bt} + \frac{e_1^{-3at-2bt}}{\mathrm{p}_{98}}\left[\begin{array}{l} \mathrm{A}_1\, e_1^{3at} + e_1^{3at+bt}\left(\mathrm{A}_2 + \mathrm{p}_{43}\mathrm{t} - \mathrm{p}_{71}\mathrm{t} + \mathrm{p}_{91}\mathrm{t}\right) + \\ \left(\mathrm{A}_3 + \mathrm{A}_6\right)e_1^{(2a+b)t} + e_1^{(2a+2b)t}\left(\mathrm{A}_4 + \mathrm{p}_{16}\mathrm{t} - \mathrm{p}_{44}\mathrm{t} + \mathrm{p}_{72}\mathrm{t}\right) \\ + \mathrm{A}_5\, e_1^{(a+2b)t} \end{array}\right] \tag{16}$$

$$\begin{aligned}
[\mathrm{H_2}]t = {} & \mathrm{H}_{2ini} + k_3\, \mathrm{c}_1\mathrm{c}_3 \frac{e_1^{-2at}}{2a} + \mathrm{c}_1\, k_3 \frac{e_1^{-(a+b)t}}{-(a+b)} - \mathrm{c}_1\mathrm{c}_2\, k_3 \frac{e_1^{-at}}{-a} + \\
& k_4\left[\mathrm{c}_3^{\,2} \frac{e_1^{-2at}}{-2a} - 2\,\mathrm{c}_3 \frac{e_1^{-(a+b)t}}{-(a+b)} + 2\,\mathrm{c}_2\mathrm{c}_3 \frac{e_1^{-at}}{-a} + 2\,\mathrm{c}_2 \frac{e_1^{-bt}}{b} - \frac{e_1^{-2bt}}{2b} + \mathrm{c}_2^{\,2}\mathrm{t}\right] \\
& + k_5\left[\mathrm{A}\frac{e_1^{-(a+b)t}}{(a+b)} + \mathrm{Ac}_3 \frac{e_1^{-2at}}{2a} - \mathrm{Ac}_2 \frac{e_1^{-at}}{-a} + \mathrm{Bc}_3 \frac{e_1^{-(a+b)t}}{(a+b)} - \mathrm{Bc}_2 \frac{e_1^{-bt}}{b} + \mathrm{B}\frac{e_1^{-2bt}}{2b}\right]
\end{aligned} \tag{17}$$

Citation: Salahuddin*, Sreelatha Devi V and Saranya K. The Kinetics of Reactions in the Mechanism of Ultraviolet Degradation of H_2S Combined with the Non-Appearance of O_2 Using the Homotopy Perturbation Method. Annal Biostat & Biomed Appli. 6(4): 2025. ABBA.MS.ID.000641. **DOI:** 10.33552/ABBA.2025.06.000641.

$$
\begin{aligned}
[\mathrm{S}]\mathrm{t} &= b\left[\mathrm{A}\frac{e_1^{-at}}{-a}+\mathrm{B}\frac{e_1^{-bt}}{-b}\right]+\mathrm{S}_{ini}+b\left[\frac{\mathrm{A}}{a}+\frac{\mathrm{B}}{b}\right] \\
&+\frac{b}{\mathrm{p}_{98}}\left[\begin{array}{l}\mathrm{A}_1\frac{e_1^{-2bt}}{-2b}-\mathrm{A}_2\frac{e_1^{-bt}}{b}+\left(\mathrm{p}_{43}-\mathrm{p}_{71}+\mathrm{p}_{91}\right)\left(\mathrm{t}\frac{e_1^{-bt}}{-b}-\frac{e_1^{-bt}}{b^2}\right)\\ +\left(\mathrm{A}_3+\mathrm{A}_6\right)\frac{e_1^{-(a+b)\mathrm{t}}}{-(a+b)}-\mathrm{A}_4\frac{e_1^{-at}}{-a}+\left(\mathrm{p}_{16}-\mathrm{p}_{44}+\mathrm{p}_{72}\right)\left(\mathrm{t}\frac{e_1^{-at}}{-a}-\frac{e_1^{-at}}{a^2}\right)\end{array}\right] \\
&+k_5\left[\mathrm{Ac}_3\frac{e_1^{-2at}}{2a}+\mathrm{Bc}_3\frac{e_1^{-(a+b)\mathrm{t}}}{(a+b)}+\mathrm{A}\frac{e_1^{-(a+b)\mathrm{t}}}{(a+b)}+\mathrm{B}\frac{e_1^{-2bt}}{2b}-\mathrm{Ac}_2\frac{e_1^{-at}}{a}-\mathrm{Bc}_2\frac{e_1^{-bt}}{b}\right] \\
&+k_6\left[\mathrm{A}^2\frac{e_1^{-2at}}{-2a}-2\,\mathrm{AB}\frac{e_1^{-(a+b)\mathrm{t}}}{(a+b)}-\mathrm{B}^2\frac{e_1^{-2bt}}{2b}\right] \qquad (18)
\end{aligned}
$$

Results and their discussions

Proposed Model of H2S Photodegradation

The cylindrical VUV lamp is placed in the centre of the photoreactor's virtualized three-dimensional representation of light intensity, with a diameter of 15 cm and a height of 14 cm, as shown in (Figure 3). The VUV lamp in the white region measures 4 cm in diameter and 5.8 cm in height, as depicted in the illustration. Figure 3 shows how the intensity of light rapidly decreases as one moves away from the light source's centre, see [12].

Major Influence Factors on H2S Photodegradation

Equations (14)-(18) represent the approximate analytical expressions for the concentrations of H_2S, H., SH., H_2, and S. Figure 3 depicts the concentration evolution of H_2S, H., SH., H_2, and S calculated 2cm away from ultraviolet light and displayed by the analytical solution (14)-(18). Figure 4 depicts influence concentration for various values (analytical) as compared to experimental results [12]. Figure 5 depicts the impact of initial gas retention and H_2S concentration duration on photodegradation rate. Constant k_3 and k_6 increased, as did the concentration of H_2S and k_{obs1} has decreased. Figure 6 shows that the simulated concentration of H. radicals increased, whereas k_{obs1}, k_1, and k_5 decreased. k_{obs2} and k_4 have increased and H. concentration decreased. Figure 7 also shows that the concentration SH. increased, k_{obs1}, k_5 increased, and k_{obs2} and k_6 decreased. Figure 8 depicts the accelerating rate of degradation. Figure 9 indicates that the simulated concentration S increased, decreased, and increased. Mathematical analysis of the simulated concentrations for the elements of H_2S photodegradation by Ultra Violet in the absence of oxygen. The concentration changes of H_2S, H., SH., H_2, and S. The model incorporates a set of steady-state non-linear reaction-diffusion equations. Applying the homotopy perturbation scheme to these equations yields analytical expressions for concentrations.

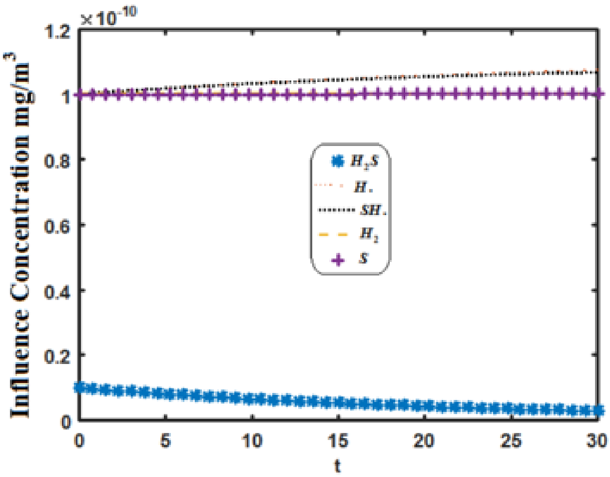

Figure 4: represents influence concentration for different values and compared experimental results.

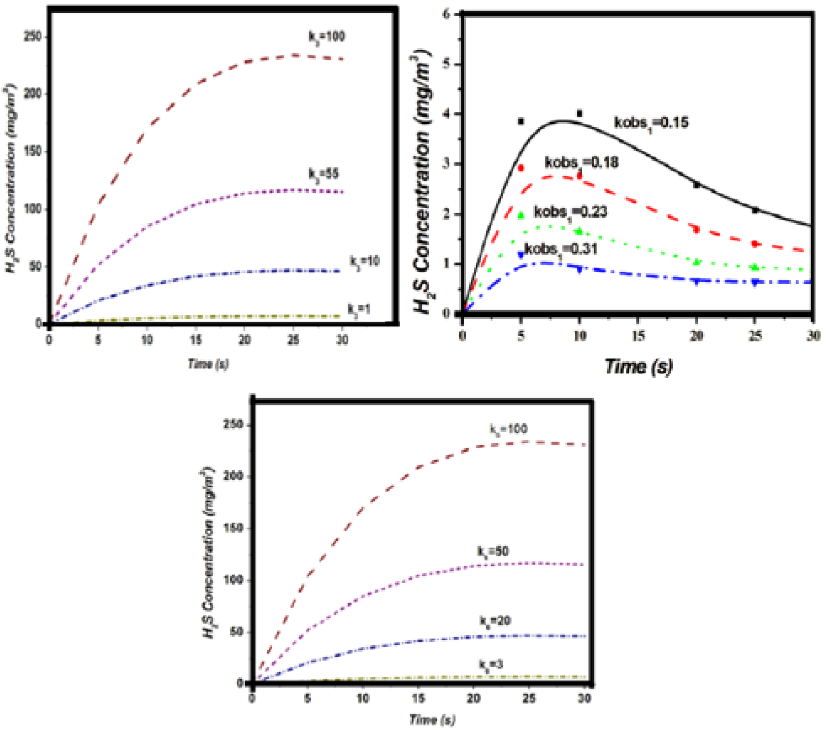

Figure 5: Plot of Influence Concentration profile versus time t computed with Equation (14) for different experimental parameter values k_{obs1}=0.15, k_{obs2}=0.00014, k3=0.2*10^2, k6=0.2*10^2.

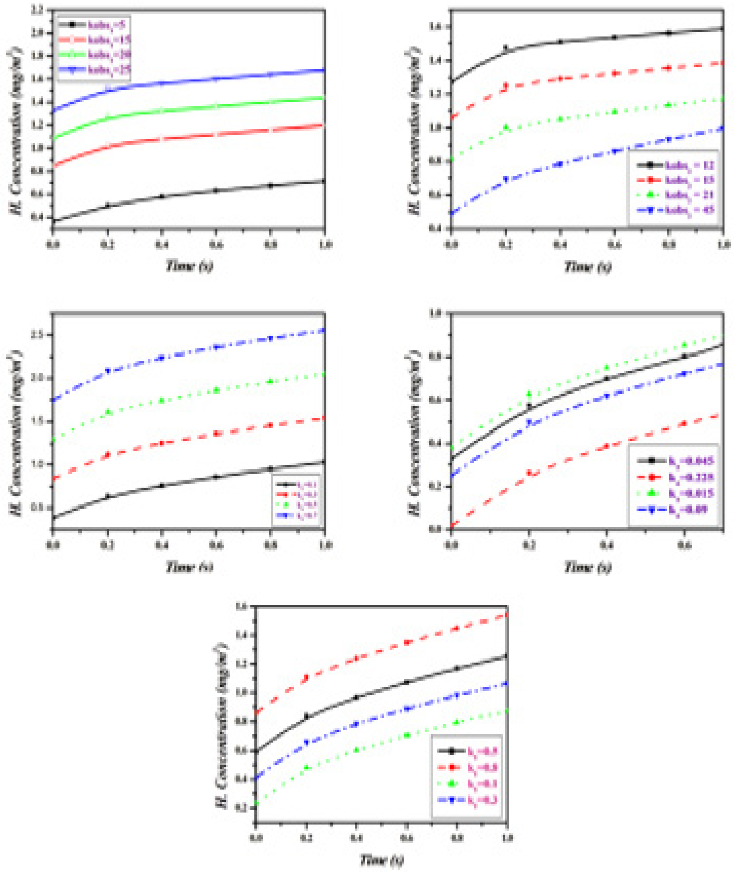

Figure 6: Plot of influence concentration profile versus time t computed with Equation (15) for different experimental parameter values k_{obs1}=5, k_{obs2}=12, k3=0.1, k4=0.045, k5=0.5.

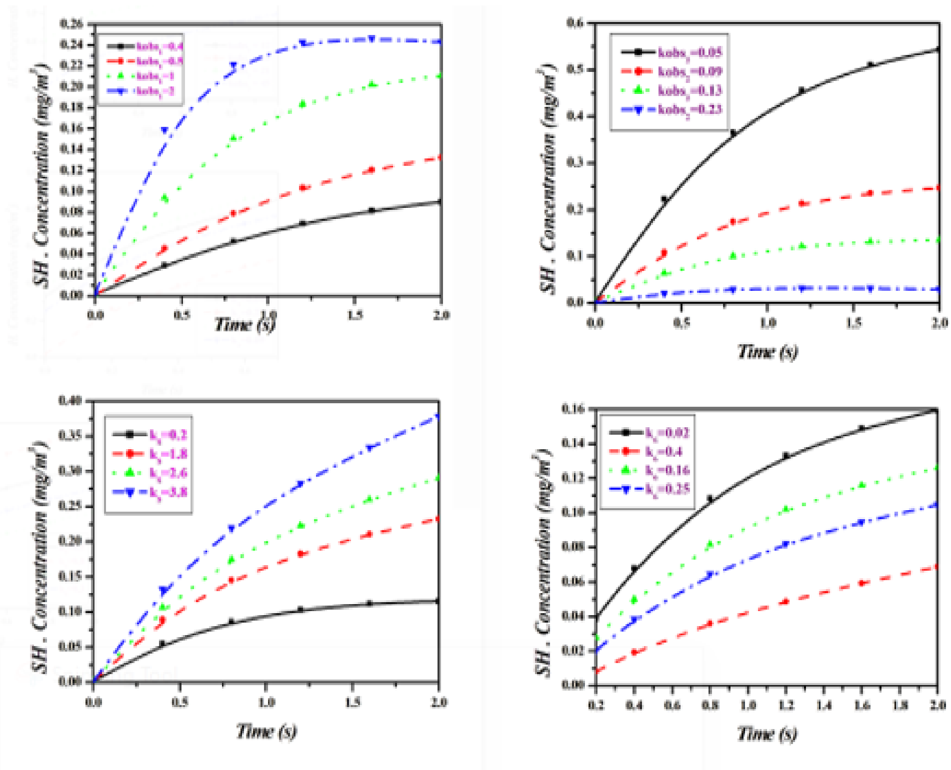

Figure 7: Plot of influence concentration profile versus time t computed with Equation (16) for different experimental parameter values k_{obs1}=0.4, k_{obs2}=0.05, k5=0.2, k6=0.02.

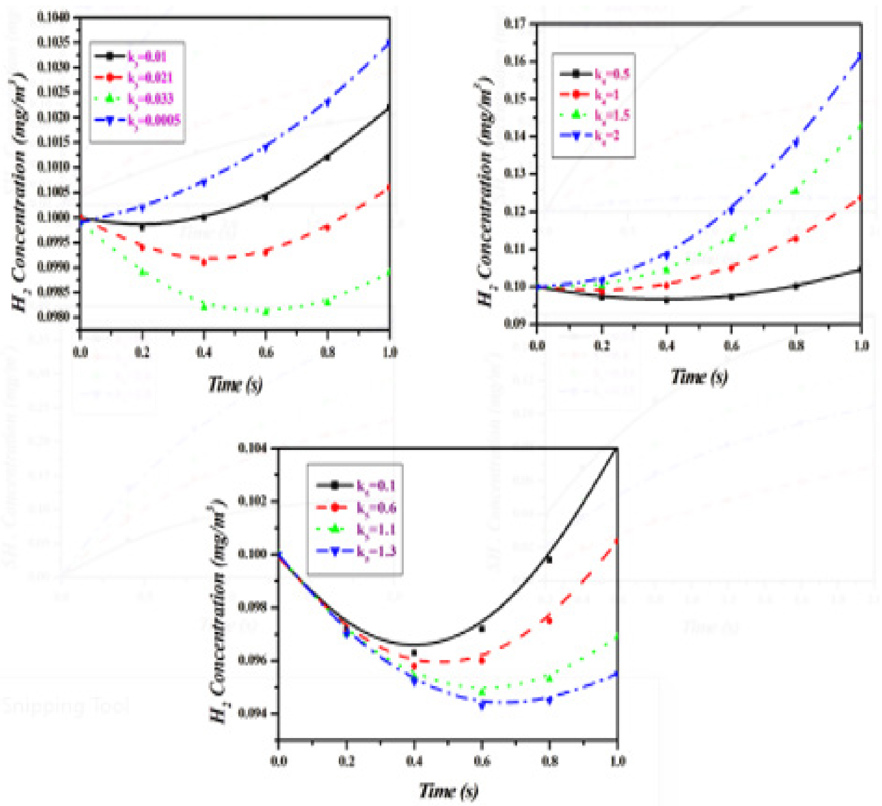

Figure 8: Plot of influence concentration profile versus time t computed with Equation (17) for different experimental parameter values k_{obs1}=1, k_{obs2}=0.1, k3=0.01, k4=0.5, k5=0.1.

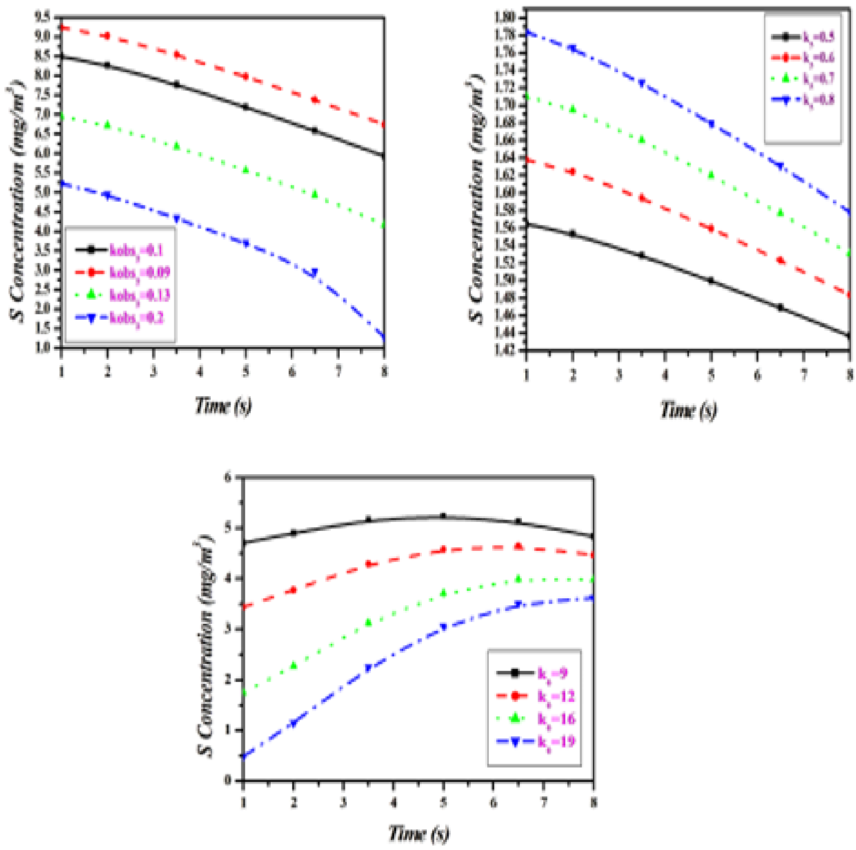

Figure 9: Plot of influence concentration profile versus time t computed with Equation (18) for different experimental parameter values k_{obs1}=1, k_{obs2}=0.1, k5=0.5, k6=9.

Conclusion

In the article's overall conclusion and future development, the proposed model of UV degradation of H_2S was determined without the presence of oxygen, and the impact of the initial H_2S concentration and gas preservation duration on the photodegradation experiment was associated with the analytical results. In this work, the nonlinear differential equations in the VUV degradation are solved analytically using HPM, and an approximate and closed analytical representation form of the concentration of H_2S, H., SH., H_2, and S is provided. These novel analytical findings provide an intuitive understanding of the system and allow parameter optimization for VUV photodegradation of H_2S in the absence of oxygen.

Conflict of interest

The authors declare no competing financial interest.

Nomenclature

Symbols	Description	Units
H_2S	Influence Concentration	mg/m^3
H.	Influence Concentration	mg/m^3
SH.	Influence Concentration	mg/m^3
H_2	Influence Concentration	mg/m^3
S	Influence Concentration	mg/m^3
k_{obs1}	Rate Constants	$m^{-1}s^{-1}$

k_{obs2}	Rate Constants	$m^{-1}s^{-1}$
k_3	Rate Constants	$m^{-1}s^{-1}$
k_4	Rate Constants	$m^{-1}s^{-1}$
k_5	Rate Constants	$m^{-1}s^{-1}$
k_6	Rate Constants	$m^{-1}s^{-1}$

Data Availability Statement

The data sets used and/or analysed during the current study are available from the corresponding author upon reasonable request.

Author's Contributions

Methodology, Validation and Investigation: K. Saranya; Resource, Visualization and Writing-Original draft: M. Suguna; Visualization, Formal Analysis and Writing-review and editing: Salahuddin. All authors have read and agreed to the published version of the manuscript.

Disclosure of Interest

No potential conflict of interest was reported by the authors.

Funding

This research is supported by the Deanship of Graduate Studies and Scientific Research at Jazan University in Saudi Arabia, under Project number GSSRD-24.

Acknowledgement

The authors gratefully acknowledge the funding of the Deanship of Graduate Studies and Scientific Research, Jazan University, Saudi Arabia, through Project Number: GSSRD-24.

References

1. Silvestre G, Fernandez B, Bonmati A (2015) Significance of anaerobic digestion as a source of clean energy in wastewater treatment plants. Energy Conversion and Management 101: 255-262.
2. Montebello AM, Mora M, López LR, Bezerra T, Gamisans X, et al. (2014) Aerobic desulfurization of biogas by acidic biotrickling filtration in a randomly packed reactor. Journal of Hazardous Materials 280: 200-208.
3. Song X, Yao W, Zhang B, Wu Y (2012) Application of Pt/CdS for the photocatalytic flue gas desulfurization. International Journal of Photoenergy.
4. Guldal NO, Figen HE, Baykara SZ (2015) New catalysts for hydrogen production from H_2S: preliminary results. International Journal of Hydrogen Energy 40(24): 7452-7458.
5. Akamatsu K, Nakane M, Sugawara T, Hattori T, Nakao S (2008) Development of a membrane reactor for decomposing hydrogen sulfide into hydrogen using a high-performance amorphous silica membrane. Journal of Membrane Science 325(1): 16-19.
6. Anani AA, Mao Z, White RE, Srinivasan S, Appleby AJ (1990) Electrochemical production of hydrogen and sulfur by low-temperature decomposition of hydrogen sulfide in an aqueous alkaline solution. Journal of the Electrochemical Society 137(9): 2703-2709.
7. Zong X, Han J, Seger B, Chen H, Lu G, et al. (2014) An integrated photoelectrochemical–chemical loop for solar-driven overall splitting of hydrogen sulfide. Angewandte Chemie 53(17): 4399-4403.
8. Bai X, Cao Y, Wu W (2011) Photocatalytic decomposition of H_2S to produce H_2 over CdS nanoparticles formed in HY-zeolite pore. Renewable Energy 36(10): 2589-2592.
9. Yan H, Yang J, Ma G, Wu G, Zong X. et al. (2009) Visible-light-driven hydrogen production with extremely high quantum efficiency on Pt–PdS/CdS photocatalyst. Journal of Catalysis 266(2): 165-168.
10. Reddy EL, Karuppiah J, Biju VM, Subrahmanyam C (2013) Catalytic packed bed non-thermal plasma reactor for the extraction of hydrogen from hydrogen sulfide. International Journal of Energy Research 37(11): 1280-1286.
11. John S, Hamann JC, Muknahallipatna SS, Legowski S, Ackerman JF, et al. (2009) Energy efficiency of hydrogen sulfide decomposition in a pulsed corona discharge reactor. Chemical Engineering Science 64(23): 4826-4834.
12. Xu JH, Ding BB, Lv XM, Lan SH, Li CL, et al. (2018) Mathematical Modeling and Mechanism of VUV Photodegradation of H_2S in the Absence of O_2. International Journal of Photoenergy.
13. Wilson SHS (1996) On the near ultraviolet photodissociation of hydrogen sulphide. Molecular Physics 88(3): 841-858.
14. Haario H, Seidman TI (1994) Reaction and diffusion at a gas/liquid interface II. SIAM Journal Mathematical Analysis 25(4): 1069-1084.
15. He JH (1999) Homotopy perturbation technique. Computational Methods Applied Mechanics Engineering 178(3-4): 257-262.
16. He JH (2000) A coupling method of a homotopy technique and a perturbation technique for nonlinear problems. Computational Methods Applied Mechanics Engineering 35(1): 37-43.
17. Saranya K, Iswarya T, Mohan V, Sathappan KE, Rajendran L (2020) Mathematical modelling of Glucose, Insulin, b -Cell Mass: Homotopy Perturbation Method Approach. European Journal of Molecular & Clinical Medicine 7(2): 3513-3530.
18. Saranya K, Mohan V, Kizek R, Fernandez C, Rajendran L (2017) Unprecedented homotopy perturbation method for solving nonlinear equations in the enzymatic reaction of glucose in a spherical matrix. Bioprocess and Biosystems Engineering 41(2): 281-294.
19. He JH (2003) Homotopy perturbation method: A new nonlinear analytical technique. Applied Mathematics Computation 135(1): 73-79.
20. He JH (2006) Homotopy perturbation method for solving boundary value problem. Physics Letters A 350(1-2): 87-88.
21. He JH (2006) Some asymptotic methods for strongly nonlinear equations. International Journal Modern Physics B 20(10): 1141-1199.
22. Kalachev LV, Seidman TL (2003) Singular perturbation analysis of a stationary diffusion/ reaction system exhibiting a corner-type behavior in the interval interior. Journal Mathematical Analysis Applications 288(2): 722-743.